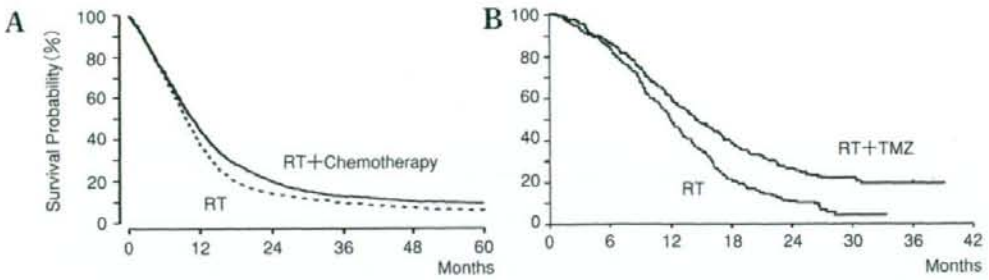

Fig. 1 Kaplan-Meier estimates of overall survival by treatment

A : A meta-analysis comparing radiotherapy (RT) and RT+chemotherapy (nitrosoureas) (modified from Stewart LA, et al).

B : Statistically significant survival advantage of patients treated by RT+temozolomide (TMZ) (modified from Stupp R, et al).

放射線照射に ACNU を併用する方法が，少数例であるがランダム化比較試験によって検証された[12]．やはり有意の生存期間延長効果は認められなかったが，腫瘍縮小率が放射線照射単独群に比べて優れていたことから，膠芽腫・退形成星細胞腫の術後治療には放射線照射と ACNU を併用する方法が，いわば community standard として広く行われることとなった．

これらの臨床試験を後追いする形で，いわゆる meta-analysis が行われた．膠芽腫・退形成性星細胞腫における術後放射線照射に化学療法を併用する治療法を検証した meta-analysis は 2 篇発表されているが[5)10)]，特に Glioma Meta-analysis Trialists Group の報告によると，12 のランダム化比較試験，3,004 例の症例を集めて解析した結果，化学療法併用による有意の生存期間延長効果が示された．この解析において p 値は 0.0001 以下であり hazard ratio (HR) は 0.85 (95%信頼区間 0.78～0.92) であった (**Fig. 1**)[10]．以上のようにして，これまでアメリカあるいはわが国では，膠芽腫・退形成性星細胞腫に対しては，術後放射線照射にニトロソウレアを併用する治療が広く行われてきた．

一般に第Ⅲ相試験における対照アームとなる治療法としては，その時点において最も生存期間の優れている「標準的治療」が用いられる．ヨーロッパでは，上述のように個々の臨床試験で放射線照射に化学療法を併用することによる生存期間延長効果が証明されていなかったことから，膠芽腫・退形成性星細胞腫に対する「標準的治療」は，術後放射線照射単独と考えられていた．したがって temozolomide と放射線照射併用に関する第Ⅲ相試験の対照アームとしては，放射線照射単独が採用された．

Temozolomide はアルキル化剤に分類される抗腫瘍薬で，血漿中など生理的条件下で容易に加水分解され，5-[(1*Z*)-3-methyltriazen-1-yl]-1*H*-imidazole-4-carboxamide (MTIC) に変換される[6]．この反応は酵素反応ではないために人種差がないと考えられているが，事実わが国において行われた薬物動態試験においても，血中濃度の動態は欧米における報告と同様であった[1]．MTIC は速やかに分解され，活性本体であるメチルジアゾニウムイオンを生成し，DNA のアルキル化分子として作用する．Temozolomide は未変化体のまま血液脳関門を通過することが確認されている[7]．そのため，temozolomide の脳腫瘍に対する効果は，血中で生成され循環する MTIC による抗腫瘍作用に加えて，未変化体の temozolomide が血液脳関門を通過し標的部位に移行した後に局所で生成される MTIC による抗腫瘍作用の両者の寄与が考えられている．

The European Organisation for Research and Treatment of Cancer (EORTC) と The National Cancer Institute of Canada は，共同で膠芽腫を対象とし術後放射線照射に temozolomide を併用する治療法を，術後放射線照射単独と比較する第Ⅲ相試験を行った[11]．Temozolomide は，照射中は 75 mg/m^{2}を連日内服，照射後は 150～200 mg/m^2 を 28 日ごとに連続 5 日間内服するサイクルを 6 サイクル行う方法で投与された．結果，放射線照射単独群と比較して，統計学的に有意の生存期間延長効果が示され，p 値は 0.001 未満，HR は 0.63 (95%信頼区間 0.52～0.75) であった．生存期間中央値は，放射線照射単独群 12.1 カ月に対して，temozolomide 併用群 14.6 カ月であった (**Fig. 1**)．Grade 3/4 の血液毒性は，放射線照射との併用時期に 7%，temozolomide 単独投与時期に 14%，またその他の有害事象のほとんどは放射線照射群と発生頻度に大きな差はなかったと報告されている．

この報告によって膠芽腫における標準的治療は，術後

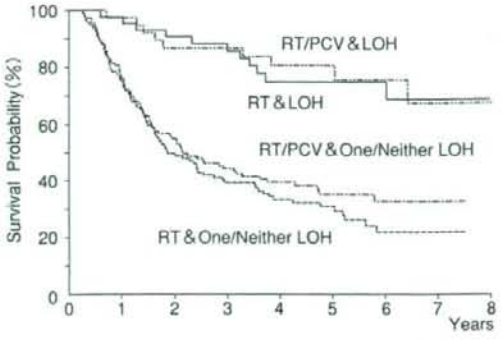

Fig. 2 Overall survival in radiotherapy (RT) and RT+PCV groups with and without combined 1p/19q loss of heterozygosity (LOH).
RT; radiotherapy, PCV; procarbazine, CCNU, and vincristine. (modified from van den Bent MJ, et al)

放射線照射と照射中ならびに照射後の temozolomide 併用となった．ただし対象アームは放射線照射単独であるので，アメリカおよびわが国で，これまで事実上の標準的治療として行われてきた放射線照射ニトロソウレア併用治療との比較を行うべきかどうかという問題が残った．これまでの標準的治療が放射線照射とニトロソウレアの併用治療であるという立場に立つのであれば，temozolomide との第Ⅲ相試験を行うべきである．これまでニトロソウレアを使用してきたのは，いわば実際的な臨床現場からの要請によるものであり，科学的には放射線照射単独が標準的治療であったという立場に立つのであれば，また前述のように meta-analysis においてもニトロソウレア併用による HR の差が 15%であるのに対して，temozolomide 併用による HR の差は 37%であり，すでにニトロソウレアとの比較は意味がないという立場に立つのであれば，次に行うべきは，temozolomide 併用放射線照射を標準的治療として，別の新規治療と比較する第Ⅲ相試験であるとも考えられる．また temozolomide と ACNU を比較する第Ⅲ相試験を行うとしても，現在，Japan Clinical Oncology Group (JCOG) の脳腫瘍研究グループが行っている放射線照射+ACNU と放射線照射+ACNU+procarbazine を比較する第Ⅲ相試験終了後に開始するのでは，およそ 5 年後のことになってしまう．これらの点については，JCOG 脳腫瘍研究グループを中心に議論が行われている最中であり，今後の動向を注目していただきたい．

退形成性乏突起膠腫に対する化学療法（PCV）の評価

退形成性乏突起膠腫が procarbazine+CCNU+vincristine (PCV) による化学療法に高い感受性を示すこと，さらにその感受性が染色体 1p と 19q の欠失の有無と相関していることは，20 世紀末の大きなトピックであった[2]．EORTC と Radiation Therapy Oncology Group (RTOG) は，別個の方法で第Ⅲ相試験を行ったが，その結果が発表された[3)14)]．両者の結果はほぼ同様であるが，RTOG のプロトコールは，放射線照射前に PCV を行う方法で行われ，PCV の dose もやや多くなっているので，ここでは放射線照射後に通常量の PCV を行っている EORTC の結果を中心に紹介し考察する．

まず，予想に反して，放射線照射に PCV を加えることによる生存期間延長効果は，いずれの試験によっても証明されなかった．しかし，再発までの期間においては，PCV を加えた群が有意に延長していた．再発後の治療は，PCV あるいは temozolomide を中心に行われていた．すなわち PCV には一定の効果が認められたが，初回治療は放射線照射単独で行い再発後に化学療法を行っても，初回から化学療法を併用しても，最終的な生存期間の観点からは同等であったということである．PCV を併用した群においては grade 3/4 の有害事象が 65%の症例でみられているので[3)]，PCV が初回から行うべき治療であるかどうかは慎重な検討を要するものと考えられる．染色体 1p と 19q の欠失の有無で解析すると，確かに染色体欠失のある群の生存期間は有意に優れていたが，これは PCV を行っても行わなくても違いがなかった (Fig. 2)．つまり，染色体欠失のある退形成性乏突起膠腫の予後が良いのは PCV が有効だからではなく，腫瘍本来の特徴であるという可能性が指摘された．

Fig. 2 には染色体欠失のない群の生存曲線も描かれているが，その生存期間中央値はおよそ 2 年と読み取れる．これは，退形成性星細胞腫における生存期間中央値とほぼ同等である．病理組織学的にも，退形成性星細胞腫と退形成性乏突起膠腫あるいは退形成性乏突起星細胞腫の区別は，神経病理学者の間においても確定していないといわれている[4)9)]．したがって，むしろこれらを「退形成性神経膠腫」として一括して扱い，「染色体欠失のある退形成性神経膠腫」と「染色体欠失のない退形成性神経膠腫」と分類したほうが臨床的には有用であるのではないかとの考え方が成り立つ可能性がある．

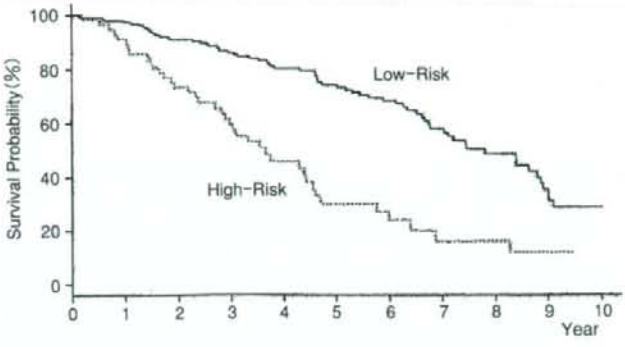

Fig. 3 Overall survival of low-grade glioma in risk groups (modified from Pignotti F, et al).

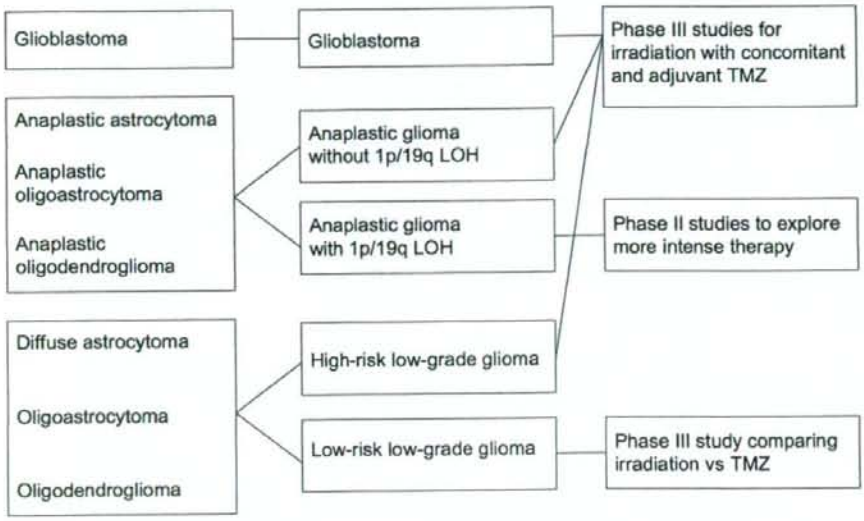

Fig. 4 Proposed treatment strategies for malignant gliomas

星細胞腫の治療をどう考えたらよいか

星細胞腫に対して放射線照射や化学療法をすべきかどうかという議論が古くから行われてきた．悪性度が低く，生存期間が長い腫瘍であるから，放射線照射はともかくとしても，化学療法は必要がないのではないかという主張がある．放射線照射については，やはり EORTC が第Ⅲ相試験を行い，放射線照射を行ったほうが再発までの期間は短いが，再発後に放射線照射を行えば最終的な生存期間では変わらないと報告している[13]．実地医療における実感として，比較的小さいうちに発見されほぼ全摘されたような腫瘍であれば，かなり長い生存期間が期待されよう．一方，いわゆる eloquent area に発生した大きな腫瘍などでは，比較的早期に悪性転化していく症例を経験する．前者のような状況であれば，照射をしないで経過をみるという選択もありえるであろうし，後者のような状況であれば，むしろ初期治療の段階から積極的に放射線照射と化学療法を行ったほうが長い生存期間を得ることができるような症例も存在するであろう．これをどのようにして判別したらよいかという疑問があった．前述の EORTC の試験のデータを用いて星細胞腫の予後因子を解析し，この疑問への解答を示唆した論文が発表されている[8]．

まず予後因子の解析から，①40 歳以上，②腫瘍径 6 cm 以上，③腫瘍が正中を越える，④組織学的に乏突起膠腫成分を含まない，⑤神経学的症状を呈する，という 5 つの予後不良因子が抽出された．次に，それぞれの因子に 1 点ずつを与え，0〜2 点の腫瘍を low-risk 群，3〜

5点の腫瘍をhigh-risk群と分類し，それぞれの生存曲線を描くと，両群はきれいに分離され，low-risk群の生存期間中央値は7.8年，high-risk群の生存期間中央値は3.67年，HR＝1.83（95％信頼区間 1.48～2.26）であった．すなわちこのhigh-risk群の生存期間は退形成神経膠腫に匹敵する（Fig. 3）．したがって，high-riskの星細胞腫・乏突起膠腫・乏突起星細胞腫は，「染色体欠失のない退形成性神経膠腫」と同様に扱って放射線照射と化学療法を行うべきであるという仮説が提唱され，これは現在欧米で検証中である．またlow-riskの星細胞腫・乏突起膠腫・乏突起星細胞腫においては，放射線照射を行う群と照射せずにtemozolomideで治療する群を比較する第III相試験がEORTCによって進行中である．

まとめ

以上に述べたようなエビデンスに基づき，臨床的見地に立った悪性神経膠腫の再分類と治療方針を図に示した（Fig. 4）．膠芽腫は放射線照射とtemozolomideの併用治療が標準的治療となり，今後はこの治療法に対して新しい治療法を比較していく方向に進むものと考えられる．退形成性乏突起膠腫に対するPCV療法は，再発までの期間を延長する効果は認められるが副作用が強く，また初期治療は放射線照射単独で行っておいて再発後に化学療法を行っても生存期間は変わらないことが示された．退形成性星細胞腫・退形成性乏突起膠腫・退形成性乏突起星細胞腫はあえて区別せずに，染色体1pと19qの欠失の有無によって，欠失のある退形成神経膠腫と染色体欠失のない退形成性神経膠腫の2群に分けて方針を立てることが提唱されつつある．前者については膠芽腫と同様の放射線照射とtemozolomide併用治療の有効性が検証中であり，後者は予後の良い疾患単位と考え，より適切で強力な治療方法が第II相試験のレベルで検証される必要があると考える．星細胞腫は，予後因子の解析からhigh-risk群とlow-risk群に分けて扱うべきであるとの考え方があり，前者はやはり膠芽腫と同様の放射線照射とtemozolomide併用治療の有効性が検証されつつあり，後者については放射線照射単独と放射線照射はせずにtemozolomide単独で治療する方法を比較する第III相試験が進行中である．

最後に，ここに示した治療方針は，あくまで確立した治療方針ではなく，今後の臨床試験の方向性を示したものであること強調しておきたい．わが国の臨床試験が，このような最先端の動向に寄与できるようなエビデンスを作ることができるようになる日を切に希望している．

文　献

1) Aoki T, Nishikawa T, Mizutani T, Nojima K, Ishikawa M, Mishima K, Adachi J, Matsutani M：Pharmacokinetics of temozolomide in the Japanese patients with relapsed glioma.（in preparation）
2) Cairncross JG, Ueki K, Zlatescu MC, Lisle DK, Finkelstein DM, Hammond RR, Silver JS, Satrk PC, Macdonald DR, Ino Y, Ramsay DA, Louis DN：Specific genetic predictors of chemotherapeutic response and survival in patients with anaplastic oligodendrogliomas. *J Natl Cancer Inst* **90**：1473-1479, 1998.
3) Cairncross G, Berkey B, Shaw E, Jenkins R, Scheithauer B, Brachman D, Buckner J, Fink K, Souhami L, Laperierre N, Mehta M, Curran W：PhaseIII trial of chemotherapy plus radiotherapy compared with radiotherapy alone for pure and mixed anaplastic oligodendroglioma：Intergroup Radiation Therapy Oncology Group trial 9402. *J Clin Oncol* **24**：2707-2714, 2006.
4) Coons SW, Johnson PC, Scheithauer BW, Yates AJ, Pearl DK：Improving diagnostic accuracy and interobserver concordance in the classification and grading of primary gliomas. *Cancer* **79**：1381-1393, 1997.
5) Fine HA, Dear KBG, Loeffler JS, Black PM, Canellos GP：Meta-analysis of radiation therapy with and without adjuvant chemotherapy for malignant gliomas in adults. *Cancer* **71**：2585-2597, 1993.
6) Newlands ES, Stevens MF, Wedge SR, Wheelhouse RT, Brock C：Temozolomide：a review of its discovery, chemical properties, pre-clinical development and clinical trials. *Cancer Treat Rev* **23**：35-61, 1997.
7) Ostermann S, Csajka C, Buclin T, Leyvraz S, Lejeune F, Decosterd LA, Stupp R：Plasma and cerebrospinal fluid population pharmacokinetics of temozolomide in malignant glioma patients. *Clin Cancer Res* **10**：3728-3736, 2004.
8) Pignatti B, van den Bent M, Curran D, Debruyne C, Sylvester R, Therasse P, Afra D, Cornu P, Bolla M, Vecht C, Karim ABMF：Prognostic factors for survival in adult patients with cerebral low-grade glioma. *J Clin Oncol* **20**：2076-2084, 2002.
9) Smith JS, Alderete B, Minn Y, Borell TJ, Perry A, Mohapatra G, Hosek SM, Kimmel D, O'Fallon J, Yates A, Feuerstein BG, Burger PC, Scheithauer BW, Jenkins RB：Localization of common deletion regions on 1p and 19q in human gliomas and their association with histological subtype. *Oncogene* **18**：4144-4152, 1999.
10) Stewart LA, Glioma meta-analysis Trialists Group：Chemotherapy in adult high-grade glioma：A systematic review and meta-analysis of individual patient data from 12 randomised trials. *Lancet* **359**：1011-1018, 2002.
11) Stupp R, Mason WP, van den Bent MJ, Weller M, Fisher B, Taphoorn MJB, Belanger K, Brandes AA, Marosi C, Bogdahn U, Curschmann J, Janzer R, Ludwin SK, Gorlia T, Allgeier A, Lacombe D, Cairncross G, Eisenhauer E, Mirimanoff RO：Radiotherapy plus concomitant and adjuvant temozolomide for glioblastoma. *N Engl J Med* **352**：987-996, 2005.
12) Takakura K, Abe H, Tanaka R, Kitamura K, Miwa T, Takeuchi K, Yamamoto S, Kageyama N, Handa H, Mogami H, Nishimoto A, Uozumi T, Matsutani M, Nomura K：Effects of ACNU and radiotherapy on malignant glioma. *J Neurosurg* **64**：53-57, 1986.
13) van den Bent MJ, Afra D, de Witte O, Ben-Hassel M,

Schraub S, Hoang-Xuan K, Malmstrom PO, Collette L, Pierart M, Mirimanoff R, Karim ABM: Long-term efficacy of early versus delayed radiotherapy for low-grade astrocytoma and oligodendroglioma in adults: The EORTC 22845 randomised trial. *Lancet* **366**: 985-990, 2005.
14) van den Bent MJ, Carpentier AF, Brandes AA, Sanson M, Taphoorn MJB, Bernsen HJJA, Frenay M, Tijssen CC, Grisold W, Sipos L, Haaxma-Reiche H, Kros JM, von Kouwenhoven MCM, Vecht CJ, Allgeier A, Lacombe D, Gorlia T: Adjuvant procarbazine, lomustine, and vincristine improves progression-free survival but not overall survival in newly diagnosed anaplastic oligodendrogliomas and oligoastrocytomas: A randomized European Organisation for Research and Treatment of Cancer phaseIII trial. *J Clin Oncol* **24**: 2715-2722, 2006.
15) Walker MD, Alexander E Jr, Hunt WE, MacCarty CS, Mahaley Ms Jr, Mealey J Jr, Norrell HA, Owens G, Ransohoff J, Wilson CB, Gehan EA, Strike TA: Evaluation of BCNU and/or radiotherapy in the treatment of anaplastic gliomas. A cooperative clinical trial. *J Neurosurg* **49**: 333-343, 1978.
16) Walker MD, Green SB, Byar DP, Alexander E Jr, Batzdorf U, Brooks WH, Hunt WE, MacCarty CS, Mahaley MS Jr, Mealey J Jr, Owens G, Ransohoff II, Robertson JT, Shapiro WR, Smith KR Jr, Wilson CB, Strike TA: Randomized comparisons of radiotherapy and nitrosoureas for the treatment of malignant glioma after surgery. *N Engl J Med* **303**: 1323-1329, 1980.

要　旨

悪性神経膠腫の治療戦略 2006

西川　亮

放射線照射に temozolomide を併用する方法を検証した第Ⅲ相試験により，初めて膠芽腫における化学療法による有意の生存期間延長効果が示された．退形成性乏突起膠腫においては，放射線照射に PCV 療法を併用する治療法は，有意の生存期間延長効果を示さなかった．また染色体 1p と 19q の欠失を有する場合は，別個の腫瘍群として扱うべきであることが示唆された．Low-grade の神経膠腫では，年齢，組織型，腫瘍径，神経学的症候などが予後因子として抽出され，これらの組合わせにより low-risk 群と high-risk 群に大別できることが示された．これらのエビデンスに基づいて，現時点における悪性神経膠腫の治療方針を考察した．

脳外誌　15：694-699，2006

J Neurosurg Pediatrics 1:148–151, 2008

Desmoplastic infantile astrocytoma and characteristics of the accompanying cyst

Case report

Takaaki Beppu, M.D.,[1] Yuichi Sato, M.D.,[1] Noriyuki Uesugi, M.D.,[2] Yasutaka Kuzu, M.D.,[1] Kuniaki Ogasawara, M.D.,[1] and Akira Ogawa, M.D., Ph.D.[1]

Departments of [1]Neurosurgery and [2]Pathology, Iwate Medical University, Morioka, Japan

✓A desmoplastic infantile astrocytoma (DIA) is an extremely rare tumor that comprises a solid astrocytic tumor accompanied by a large cyst and involves the superficial cerebral cortex and leptomeninges in infants. The solid part of this type of tumor has been well described in various reports and books, but characteristics of the cystic portion have remained unclear. Because adequate resection is required to ensure a favorable prognosis, information about the cyst is very important for diagnostic purposes and surgical planning. The authors report on the clinical and histological features of the cyst in a case of a DIA. A 12-month-old boy presented with vomiting. Contrast-enhanced magnetic resonance imaging revealed a strongly enhancing single-lobed large cyst located in the deep white matter, under the solid part of the tumor attached to the dura mater of the left frontal lobe. Both the solid and cystic portions of the tumor were surgically removed. The border between the cyst wall and surrounding white matter was unclear. Histologically, the cyst wall was composed of gliosis representing a rough accumulation of reactive astrocytes, lymphocytes, and small capillary vessels in edematous parenchyma, but no tumor cells. The present case and previous reports suggest that the cyst does not contain tumor cells, even if strongly depicted on contrast-enhanced neuroimaging, and that a thickly enhancing cyst wall indicates gliosis with accumulation of numerous small vessels. *(DOI: 10.3171/PED/2008/1/2/148)*

Key Words • **cyst** • **desmoplastic infantile astrocytoma** • **desmoplastic infantile ganglioglioma** • **histology** • **magnetic resonance imaging** • **pediatric neurosurgery**

A DIA, originally referred to as a "superficial cerebral astrocytoma attached to dura with desmoplastic reaction" or "desmoplastic cerebral astrocytoma of infancy," has been defined as a large cystic astrocytic tumor in infants that involves the superficial cerebral cortex and leptomeninges, often attaching to the dura mater, with a generally good prognosis following adequate resection.[21,22] Both a DIA and a DIG have been integrated into the same tumor type class in the World Health Organization classification system, as both tumors display similar clinical and pathological features, excluding involvement of a variable neuronal component together with astrocytes in a DIG.[21] The solid part of the tumor is easily removed due to the location and clear demarcation from surrounding brain tissue.[20] Because surgical removal of the tumor leads to favorable prognosis, neurosurgeons play a large role in the treatment of a DIA and DIG. Although both a DIA and DIG are very rare, characteristics of the solid part of the tumor have been well described.[4,17,22] In contrast, characteristics of the cyst have remained unclear. For neurosurgeons, general information on clinical and histopathological features of the cyst is important for diagnosis and treatment. The current report describes a case of a DIA with a large cyst, and reviews clinical and histological findings of DIA cysts in the literature.

Abbreviations used in this paper: DIA = desmoplastic infantile astrocytoma; DIG = desmoplastic infantile ganglioglioma; MR = magnetic resonance.

Case Report

History and Examination. This 12-month-old boy was born at term after an uncomplicated pregnancy and delivery. His perinatal course was normal. One month before admission, he presented with vomiting. On admission, an examination revealed a head circumference of 50.3 cm (greater than the mean plus 2 standard deviations) but no neurological deficits. His medical history included no episodes suggestive of

systemic autoimmune disease, intracranial infection, or head injury, and revealed no previous surgery or radiation treatment. Physical and blood serum examinations revealed no abnormalities.

Magnetic resonance was performed, and T1- and T2-weighted imaging revealed a circumscribed solid lesion located superficially in the cortex of the left frontal lobe, and a large cyst in the deep white matter medial to the solid tumor. The T1- and T2-weighted imaging also showed isointense and very low signals, respectively. Gadolinium-enhanced T1-weighted imaging revealed homogeneous enhancement in the solid part of the tumor with the exception of the central region (Fig. 1). A large single-lobed cyst (maximum diameter 5.5 cm) accompanied the solid part of the tumor. Fluid in the cyst displayed greater signal intensity than cerebrospinal fluid. The thick cyst wall also displayed strong enhancement on gadolinium-enhanced T1-weighted imaging (Fig. 1). Computed tomography depicted no calcified foci in the solid part of the tumor or in the cyst wall. Left internal carotid angiography revealed slight intratumoral neovascularity fed from the operculum artery, whereas no intratumoral neovascularity was found on external carotid angiography.

Operation and Postoperative Course. A skin incision and craniotomy were performed at the region of presumed exposure of the tumor. Before opening the dura, xanthochromic fluid in the cyst was aspirated using ultrasonographic guidance until sufficient relaxation of the frontal lobe was achieved. Upon opening, the dura did not firmly adhere to the solid part of the tumor. The meningioma-like hard and reddish-gray solid portion was well demarcated due to preservation of arachnoid matter adjacent to the tumor, and was easily separated from surrounding cortex and edematous white matter. After removal of the solid portion, the cyst wall was noted to consist of a soft and gliotic membrane with a reddish-gray color. Although the cyst could be removed completely, separation of the cyst wall from surrounding white matter was more difficult than removal of the solid portion, because the border between the cyst wall and surrounding white matter was unclear. We dissected between the cyst and surrounding white matter using an ultrasonic surgical aspirator. Postoperative MR imaging demonstrated that both the solid and cystic portions of the tumor had been completely removed.

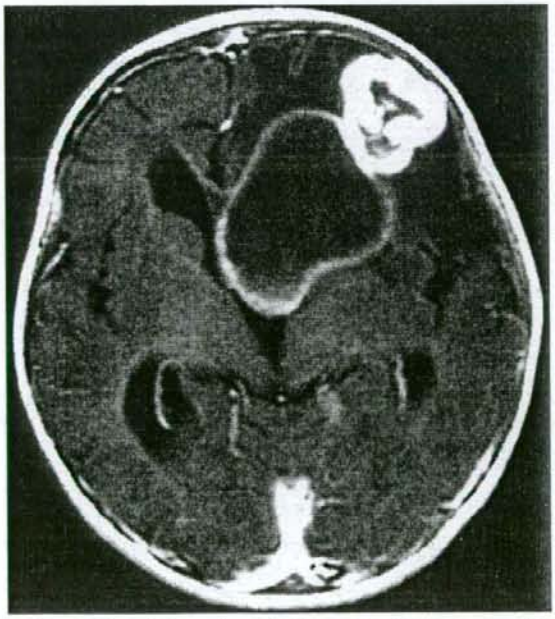

FIG. 1. Gadolinium-enhanced T1-weighted MR image reveals a heterogeneous enhancing mass attached to the dura in the left frontal convex. The mass accompanies a large and thickly enhancing cyst in the deep white matter.

Histology. The removed solid part of the tumor revealed typical histological features of proliferating spindle-shaped cells intermingling with large amounts of collagenous stroma showing storiform or whorled patterns (Fig. 2 *upper*). The collagenous stroma displayed positive results for silver staining. Spindle-shaped cells were immunohistochemically positive for glial fibrillary acidic protein. No necrosis, mitosis, calcified focus, or synaptophysin-positive ganglion cells were seen anywhere in the tumor. The histological diagnosis of the tumor was a DIA.

The cyst wall demonstrated histological features of gliosis, with numerous small round cells such as astrocytes and lymphocytes, and numerous small vessels scattered in edematous parenchyma. Reactive gliosis was observed in the surrounding white matter (Fig. 2 *lower*). In particular, small vessels had accumulated close to the outside of the cyst wall. The cyst wall and brain tissue adjacent to the tumor were thoroughly positive for glial fibrillary acidic protein. Examination of the entire cyst wall, however, revealed no tumor cells.

Discussion

The DIA and DIG tumor types are extremely rare. Only 31 cases of a DIA have been reported in the literature.[1,3,5–19,21,22,24] The tumor was accompanied by a cyst in 30 of 32 cases (93.8%), including the present case. The DIA comprised a solid tumor without a cyst in only 2 cases.[8,18] Cyst size was defined in 15 cases from 9 reports (including the present study) and varied widely between 1.5 and 12 cm (mean 9.3 cm). The cyst in a DIA is most frequently composed of a single lobule on preoperative neuroimaging as in the present case, rather than multiple lobules separated by septa. Reports have described cysts with 1, 2, and 3 lobules in 10, 3,[7,16,17] and 2 cases,[14,19] respectively. The solid part of a DIA is frequently located at the superficial cerebrum, and the cyst has been located in the deep cerebrum under the solid portion in almost all previous cases. In 19 cases for which cyst location was defined,[1,3,6,7,9,10,13–17,19,21,22,24] only 3 cases revealed the cyst to be in a location other than deep white matter medial to the solid part of the tumor.[10,19,24]

The cyst in the present case possessed a thick wall in addition to strong enhancement on gadolinium-enhanced T1-weighted imaging. Results from previous studies, however, have suggested that the cyst wall was obscure and lacked enhancement on contrast-enhanced computed tomography scans or MR images.[19,23] In the literature, 15 reports have described findings on contrast-enhanced computed tomography scans or MR images, with 11 cases demonstrating

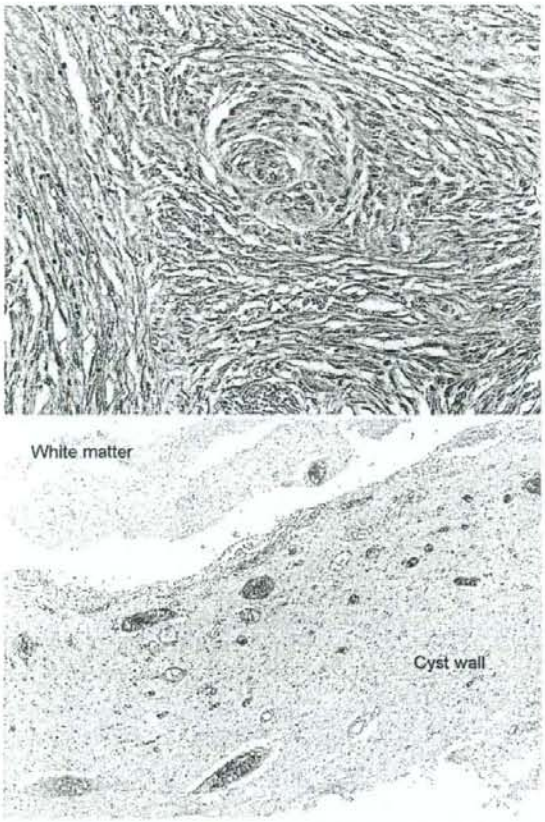

FIG. 2. Photomicrographs of the histological features of the solid *(upper)* and cystic *(lower)* portions of the tumor. *Upper:* The solid part of the tumor displays typical histological features with proliferation of spindle-shaped cells intermingling with a large amount of collagenous stroma showing storiform or whorled patterns. *Lower:* The cyst wall displays scattered small round cells such as astrocytes and lymphocytes, and small capillary vessels in edematous parenchyma. White matter adjacent to the cyst also demonstrates the same round cells. Capillary vessels are accumulated more in the outer cyst wall. H & E, original magnification × 100 *(upper)* and × 40 *(lower)*.

obscure or unenhanced cyst walls and 4 cases showing thickly enhancing cyst walls.[6,11,14,17] The cyst wall in the present case did not contain tumor cells in sections stained using H & E. Some reports have described histological features of the cyst wall. Kurose and coauthors[10] reported that a thickly enhancing cyst wall in a case of DIA did not contain tumor cells but showed scattered xanthoma cells with normal morphological features. Sugiyama and associates[20] reported 4 cases in a mixed series of DIA and DIG cases, and also noted that cyst walls were free of invading tumor cells. Kim et al.[7] observed no tumor cells within the septum of a multilobular cyst in a case involving a DIA. No reports have found tumor cells in the cyst wall of a DIA. An obscure and nonenhancing cyst wall in a DIA case showed macroscopically gliotic characteristics during surgery according to de Chadarévian and coworkers.[3] In the present case, macroscopic observation of the cyst wall revealed gliotic characteristics during surgery, and the cyst wall histologically demonstrated the features of gliosis, with numerous scattered round cells such as astrocytes and lymphocytes, and small vessels in edematous parenchyma. We speculate that enhancement of the cyst wall on neuroimaging is induced by accumulation of the small vessels within the area of gliosis, or increasing permeability of the blood–brain barrier in vessels due to gliosis. Kandalkar and colleagues[5] reported that the histology of the cyst wall in a case of a DIA showed normal but atrophic brain tissues in which the outer layer was increased due to gliosis, although results of neuroimaging were not demonstrated. They speculated that these histological changes in the cyst resulted from pressure of cyst fluid on the adjacent brain, and recommended excision of the cyst portion for seizure control after surgery. In the present case, gliosis was increased within the outer cyst wall, and was observed in adjacent white matter tissue. The border between the cyst wall and surrounding white matter was unclear. This adhesion between the cyst wall and surrounding white matter might be induced by aggressive gliosis within the outer side of the wall. The deep location, large size, and unclear border of the cyst may complicate removal of the cystic portion compared with the solid portion. Gross-total removal of a DIA or DIG leads to a favorable prognosis, but long-term survival is anticipated even with residual disease.[21,22] It needs to be emphasized that surgery for DIA only requires removal of the solid portion of the tumor when the cyst wall is nonenhanced on neuroimaging. This approach is similar to the surgical plan for a pilocytic astrocytoma, in which neurosurgeons generally assume that the cyst wall is not neoplastic or does not require resection.[2] Based on findings from the present case and the literature, we also believe that surgery for a DIA with a thickly enhancing cyst wall only requires removal of the solid portion of the tumor and that removal of the cyst wall is not necessary. If the residual cyst wall causes uncontrollable seizures after surgery, a second operation to remove the cyst wall should be considered.

Conclusions

Cyst characteristics of a DIA or DIG do not appear to have been fully explored in previous studies. Because surgery plays a large role in treatment for a DIA and DIG, characteristics of the cyst commonly located in the deep white matter under the solid part of the tumor represent important information for neurosurgeons. Clinical and histological findings in the present case and previous reports suggest that the cyst does not contain tumor cells, even if strong enhancement is seen on contrast-enhanced neuroimaging, and that a thickly enhancing cyst wall indicates gliosis with accumulation of numerous small vessels. The border between the cyst wall and surrounding white matter is unclear compared with the border between the solid portion and surrounding cortex. We therefore believe that the cyst wall does not require removal during surgery for a DIA, even when the cyst wall is thickly enhanced on neuroimaging. Further study of the cyst wall in a limited group of patients with a DIA or DIG is required to confirm our distinct impressions.

Acknowledgment

We thank Prof. Shinichi Nakamura of the Department of Pathology, Iwate Medical University, for performing the histological examination in the present case.

References

1. Aydin F, Ghatak NR, Salvant J, Muizelaar P: Desmoplastic cerebral astrocytoma of infancy. A case report with immunohistochemical, ultrastructural and proliferation studies. **Acta Neuropathol (Berl) 8:**666–670, 1993
2. Burger PC, Scheithauer BW, Paulus W, Szymas J, Giannini C, Kleihues P: Pilocytic astrocytoma, in Kleihues P, Cavenee WK (eds): **World Health Organization of Tumours. Pathology and Genetics: Tumours of the Nervous System.** Lyon: IARC Press, 2000, pp 45–51
3. de Chandarévian JP, Pattisapu JV, Faerber EN: Desmoplastic cerebral astrocytoma of infancy. Light microscopy, immunocytochemistry, and ultrastructure. **Cancer 66:**173–179, 1990
4. Grundy R, Mallucci C: Rare tumors, in Walker DA, Perilongo G, Punt JAG, et al (eds): **Brain and Spinal Tumors of Childhood.** London: Arnold, 2004, pp 397–416
5. Kandalkar B, Shah V, Shet T: Desmoplastic astrocytoma of infancy—a case report. **Indian J Pathol Microbiol 44:**329–332, 2001
6. Kato M, Yano H, Okumura A, Shinoda J, Sakai N, Shimokawa K: A non-infantile case of desmoplastic infantile astrocytoma. **Childs Nerv Syst 20:**499–501, 2004
7. Kim JH, Kim IO, Kim WS, Kim KH, Park CM, Yeon KM: MR findings of desmoplastic cerebral astrocytoma of infancy. **Acta Radiol 44:**688–690, 2003
8. Kopniczky Z, Kóbor J, Maráz A, Vajtai I: Desmoplastic neuroepithelial tumor of infancy in the nevus sebaceus syndrome: report of a unique constellation and review of the literature. **Pathol Res Pract 197:**279–284, 2001
9. Kros JM, Delwel EJ, de Jong TH, Tanghe HL, van Run PR, Vissers K, et al: Desmoplastic infantile astrocytoma and ganglioglioma: a search for genomic characteristics. **Acta Neuropathol (Berl) 104:**144–148, 2002
10. Kurose A, Beppu T, Miura Y, Suzuki M, Ogawa A, Arai H, et al: Desmoplastic cerebral astrocytoma of infancy intermingling with atypical glial cells. **Pathol Int 50:**744–749, 2000
11. Louis DN, von Deimling A, Dickersin GR, Dooling EC, Seizinger BR: Desmoplastic cerebral astrocytomas of infancy: a histopathologic, immunohistochemical, ultrastructural, and molecular genetic study. **Hum Pathol 23:**1402–1409, 1992
12. Mallucci C, Lellouch-Tubiana A, Salazar C, Cinalli G, Renier D, Sainte-Rose C, et al: The management of desmoplastic neuroepithelial tumors in childhood. **Childs Nerv Syst 16:**8–14, 2000
13. Olas E, Kordek R, Biernat W, Liberski PP, Zakrzewski K, Alwasiak J, et al: Desmoplastic cerebral astrocytoma of infancy: a case report. **Folia Neuropathol 36:**45–51, 1998
14. Park K, Yoo J, Cho H, Cho W, Park S: Desmoplastic cerebral astrocytoma of infancy: a case report. **J Korean Med Sci 13:** 440–444, 1998
15. Paulus W, Schlote W, Perentes E, Jacobi G, Warmuth-Metz M, Roggendorf W: Desmoplastic supratentorial neuroepithelial tumors of infancy. **Histopathology 21:**43–49, 1992
16. Rodriguez-Morales EL, Correa Rivas MS, Colon CE: Desmoplastic astrocytoma of infancy: a case report with histopathologic and immunohistochemistry profile. **P R Health Sci J 21:** 129–132, 2002
17. Rosenblum MK: Desmoplastic infantile astrocytoma/desmoplastic infantile ganglioglioma, in McLendon RE, Rosenblum MK, Bigner DD (eds): **Russell and Rubinstein's Pathology of Tumors of the Nervous System, ed 7.** London: Hodder Arnold, 2006, pp 321–332
18. Rushing EJ, Rorke LB, Sutton L: Problems in the nosology of desmoplastic tumors of childhood. **Pediatr Neurosurg 19:**57–62, 1993
19. Serra A, Strain J, Ruyle S: Desmoplastic cerebral astrocytoma of infancy: report and review of the imaging characteristics. **AJR Am J Roentgenol 166:**1459–1461, 1996
20. Sugiyama K, Arita K, Shima T, Nakaoka M, Matsuoka T, Taniguchi E, et al: Good clinical course in infants with desmoplastic cerebral neuroepithelial tumor treated by surgery alone. **J Neurooncol 59:**63–69, 2002
21. Taratuto AL, Monges J, Lylyk P, Leiguarda R: Superficial cerebral astrocytoma attached to dura. Report of six cases in infants. **Cancer 54:**2505–2512, 1984
22. Taratuto AL, VandenBerg SR, Rorke LB: Desmoplastic infantile astrocytoma and ganglioglioma, in Kleihues P, Cavenee WK (eds): **World Health Organization of Tumours. Pathology and Genetics: Tumours of the Nervous System.** Lyon: IARC Press, 2000, pp 99–102
23. Trehan G, Bruge H, Vinchon M, Khalil C, Ruchoux MM, Dhellemmes P, et al: MR imaging in the diagnosis of desmoplastic infantile tumor: retrospective study of six cases. **AJNR Am J Neuroradiol 25:**1028–1033, 2004
24. Vajtai I: Desmoplastic cerebral astrocytoma in intraventricular location: simplifying histogenesis by broadening the spectrum of desmoplastic neuroepithelial tumors of infancy? **AJR Am J Roentgenol 168:**1385, 1997

Manuscript submitted July 29, 2007.
Accepted September 26, 2007.
This work was supported by the Advanced Medical Science Center, Iwate Medical University, Morioka, Japan.
Address correspondence to: Takaaki Beppu, M.D., Department of Neurosurgery, Iwate Medical University, 19-1 Uchimaru, Morioka 020-8505, Japan. email: tbeppu@iwate-med.ac.jp.

ELSEVIER

Clinical Neurology and Neurosurgery 109 (2007) 106–110

Clinical Neurology and Neurosurgery

www.elsevier.com/locate/clineuro

Case report

Diffusion tensor imaging for differentiation of recurrent brain tumor and radiation necrosis after radiotherapy—Three case reports

Hiroshi Kashimura *, Takashi Inoue, Takaaki Beppu, Kuniaki Ogasawara, Akira Ogawa

Department of Neurosurgery, Iwate Medical University School of Medicine, 19-1 Uchimaru, Morioka, Iwate, Japan

Received 26 October 2005; received in revised form 24 March 2006; accepted 3 April 2006

Abstract

Fractional anisotropy (FA) is influenced by histological data such as cellularity, vascularity and/or fiber structure in astrocytic tumors. We describe two patients with tumor recurrence and one patient with radiation necrosis who were diagnosed using assessment of FA value. The assessment of FA value in enhanced lesions after radiotherapy may be able to differentiate radiation necrosis from tumor recurrence.

Keywords: Fractional anisotropy; Diffusion tensor imaging; Tumor recurrence; Radiation necrosis

1. Introduction

A differential diagnosis between tumor recurrence and radiation necrosis is difficult after radiotherapy of brain tumors using contrast-enhanced magnetic resonance (MR) imaging. Damage to the blood–brain barrier induced by radiation results in leakage of gadolinium into the interstitium, which produces a ring-enhancing lesion that can mimic tumor recurrence [1]. Several accepted methods for non-invasively differentiating tumor recurrence from radiation necrosis are available, including positron emission tomography (PET), single-photon emission computed tomography (SPECT) and ^{1}H MR spectroscopy [2–8]. However, using [^{18}F]fluorodeoxyglucose or L-[methyl-^{11}C]methionine-PET scanning, a differential diagnosis was occasionally difficult in several low-grade gliomas with hypometabolism or necrotic areas secondary to radiation therapy [9,10]. Using ^{201}thallium (^{201}Tl)-SPECT scanning, increased ^{201}Tl uptake was observed in both radiation necrosis and inflammatory infectious processes [11]. ^{1}H MRS allow reliable differential diagnostic statements to be made when the tissues are composed of either pure tumor or pure necrosis, however spectral patterns are less definitive when tissues composed of varying degrees of mixed tumor and necrosis are examined [8].

Recently, diffusion tensor (DT) imaging has been developed to obtain quantitative information regarding the magnitude and directionality of water diffusion [12–16]. Several indices, such as the fractional anisotropy (FA), the relative anisotropy (RA) and the volume ratio (VR) are derived from DT imaging. A comparative study of FA, RA and VR in cat brain demonstrated that FA can precisely measure the degree of deviation from isotropic diffusion [17], and provides the best performance in terms of contrast-to-noise ratio as a function of signal-to-noise ratio in simulations [18,19]. FA value is expressed as numerical value between 0 and 1 without a unit. FA of 0 corresponds to unrestricted isotropic diffusion and 1 corresponds to linear anisotropic diffusion of water. FA was influenced by histological data such as cellularity, vascularity and/or fiber structure in astrocytic tumors [13]. We describe two patients with tumor recurrence and one patient with radiation necrosis who were diagnosed using assessment of the FA values.

2. Case reports

2.1. MR imaging and image analysis

All scans were performed using a Signa VH/i 3.0 T scanner (General Electric Systems, Milwaukee, Wis.) and standard head coil. A spine echo type echo planar imaging sequence

* Corresponding author. Tel.: +81 19 651 5111; fax: +81 19 625 8799.
E-mail address: hkashi@iwate-med.ac.jp (H. Kashimura).

0303-8467/$ – see front matter © 2006 Elsevier B.V. All rights reserved.
doi:10.1016/j.clineuro.2006.04.005

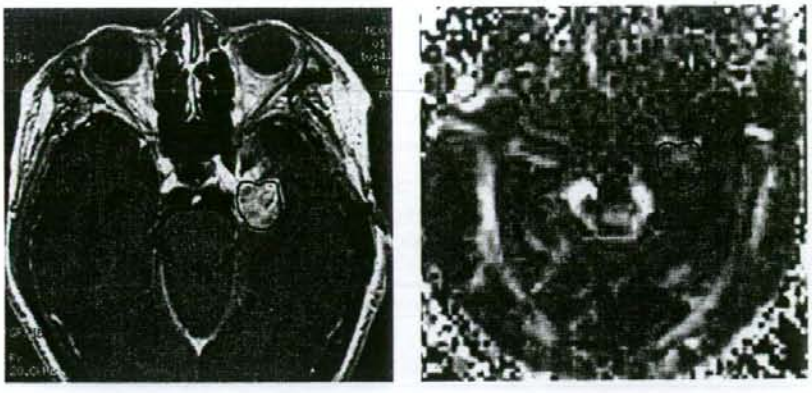

Fig. 1. Left: T1-weighted magnetic resonance (MR) image with contrast medium showing the region of interest (ROI) in the solid portion of the lesion. Right: fractional anisotropy map showing the outline of the ROI traced automatically.

with diffusion gradients applied in six directions was used for the diffusion tensor imaging with the following parameters: repetition time (TR); 10,000 ms, echo time (TE); 84 ms, slice thickness; 6 mm, field of view (FOV); 240 mm^2, matrix; 256 × 260, 2 mm gap and b factors, 800 s/mm^2. Fast spin echo T1- and T2-weighted imaging were performed prior to DT imaging, and T1-weighted with contrast medium was performed after DT imaging.

The FA value was calculated using a subprogram of the Functool™ image analysis software (General Electric Medical Systems, Buc, France). One large region of interest (ROI) was placed within enhanced region on a T1-weighted contrast medium image. ROI was automatically transferred onto the co-registered FA maps constructed from DT imaging. The FA values were then calculated for each patient using the Functool™ image analysis software. The FA value was identified as a mean of values derived for every pixel in a given ROI.

2.1.1. Case 1

A 67-year-old woman had been treated for left anaplastic astrocytoma by surgical resection, radiation and chemotherapy. Eleven months after the initial treatment, follow-up gadolinium-enhanced T1-weighted MR imaging revealed an enlarged enhanced lesion (Fig. 1, left). ROI was placed within enhanced region. The FA value of the enhanced lesion was 0.27 ± 0.04 on the FA map (Fig. 1, right). The lesion was as diagnosed tumor recurrence. The patient underwent craniotomy and then total resection. Histological examination revealed a glioblastoma.

2.1.2. Case 2

A 56-year-old woman had been treated for left frontal astrocytoma by surgical resection, radiation and chemotherapy. Seventeen months after the initial treatment, follow-up MR imaging showed an enlarged enhanced lesion (Fig. 2, left). ROI was placed within enhanced region. The FA

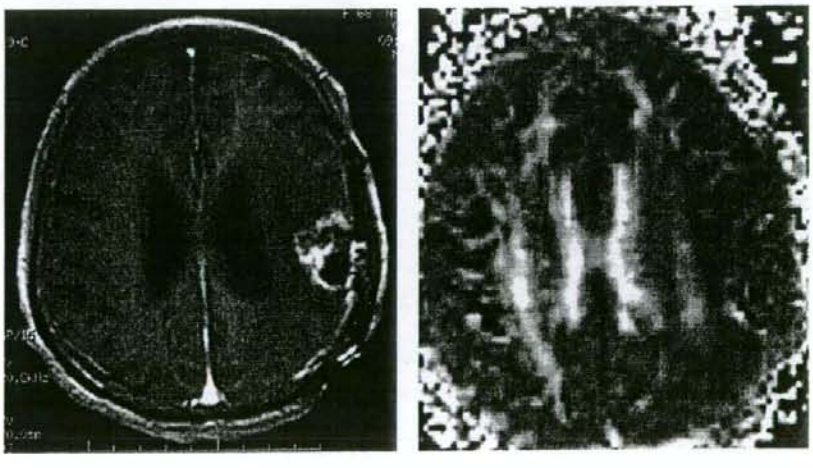

Fig. 2. Case 1—images obtained from a 67-year-old woman. Left: T1-weighted magnetic resonance images with gadolinium revealing heterogeneously enhanced lesions with operative scar in the left parietal lobe. Right: co-registered FA maps from DTI. The FA value was 0.27 ± 0.04.

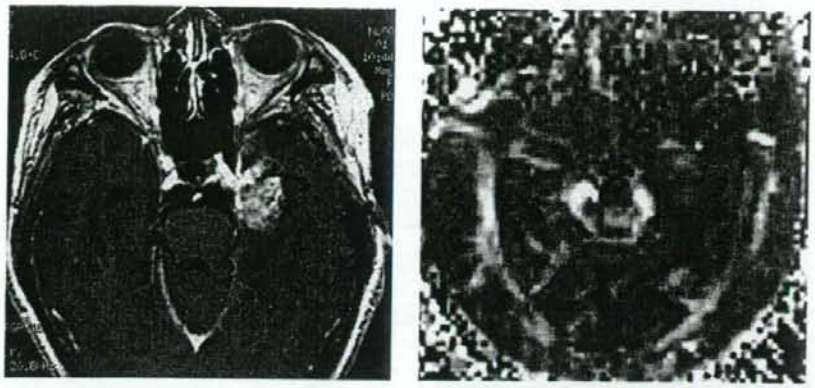

Fig. 3. Case 2—images obtained from a 56-year-old woman. Left: T1-weighted magnetic resonance images with gadolinium revealing massive enhanced lesions in the left temporal lobe. Right: co-registered FA maps from DT imaging. The FA value was 0.29 ± 0.04.

value of the enhanced lesion was 0.29 ± 0.04 (Fig. 2, right). The patient underwent craniotomy and then total resection. Histological examination revealed features of glioblastoma.

2.1.3. Case 3

A 44-year-old man had been treated for right frontal oligoastrocytoma by surgical resection, radiation and chemotherapy. Twenty-four months after the initial treatment, follow-up MR imaging revealed an enlarged enhanced lesion (Fig. 3, left). ROI was placed within enhanced region. The FA value of the enhanced lesion was 0.17 ± 0.03 (Fig. 3, right). The patient underwent craniotomy and then total resection. Histological examination revealed radiation necrosis (Fig. 4).

3. Discussion

DT imaging can predict the structural properties of tissue, such as the integrity and orientation of tracts in the brain [20,21]. The FA values in normal white matter show strong directionality of water diffusion, and consequently a high FA value, as water diffusion parallel to the white matter tracts is less restricted than water diffusion perpendicular to them [22]. On the other hand, in astrocytic tumors, almost all normal fibers and cell structures are destroyed by the tumor nidus, or displaced, separating to surround the tumor nidus [23]. These changes may be one cause of the observed decrease in the directionality of water diffusion and decreased FA values [13]. The FA values are influenced not only by tissue damage, but also histologi-

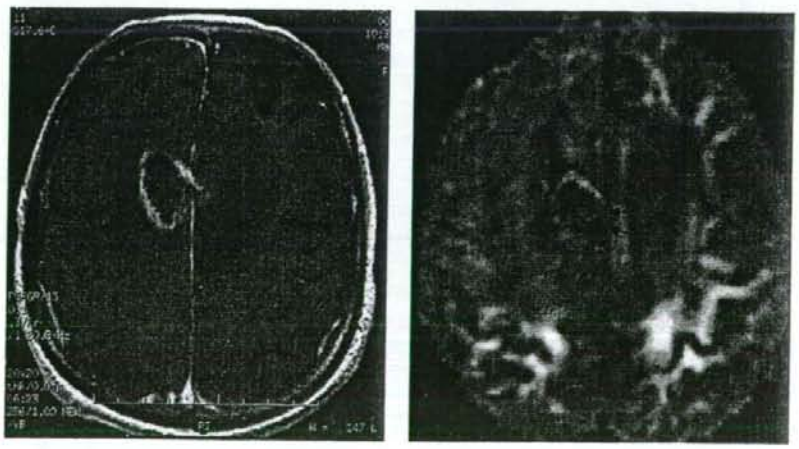

Fig. 4. Case 3—images obtained from a 44-year-old man. Left: T1-weighted magnetic resonance images with gadolinium revealing heterogeneously enhanced lesions with operative scar in the right frontal lobe. Right: co-registered FA maps from DT imaging. The FA value was 0.17 ± 0.03. Arrows show the area of decreased FA value on the enhanced region.

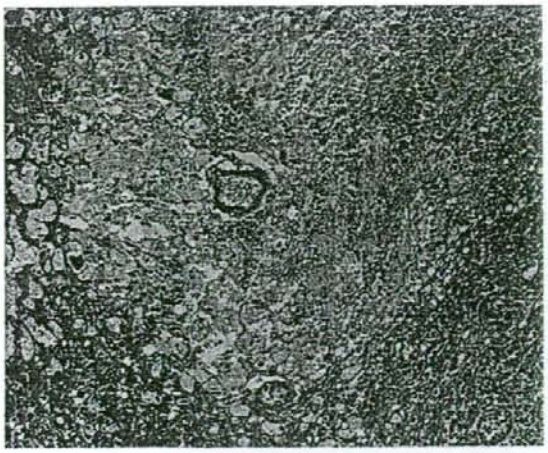

Fig. 5. Microscopic findings obtained from case 3. Lower-power view showing hyalinized tissue and reactive glia, H and E.

cal characteristics such as cellularity, vascularity and/or fiber structure, and this correlation thereby leads to a tendency for tumors of higher grade to present with higher FA values [12,13,16].

The relationship between the FA value and each histological type of astrocytic tumors has been reported, with mean FA values of 0.24 ± 0.06 in glioblastoma, 0.19 ± 0.06 in anaplastic astrocytomas, 0.12 ± 0.02 in diffuse astrocytomas and 0.16 ± 0.02 in pilocytic astrocytomas [12]. A relationship between FA value and the WHO classification of gliomas has also been reported. The FA value of grade 1 gliomas (0.150 ± 0.017) is significantly lower than that of grade 3 (0.23 ± 0.033) or grade 4 (0.229 ± 0.033) gliomas. The FA value of grade 2 gliomas (0.159 ± 0.018) is significantly lower than those of grade 3 or 4 gliomas [16]. In our cases, the FA values of recurrent tumor were 0.27 ± 0.04 and 0.29 ± 0.04, which are equivalent to the previously reported FA value of primary gliomas. These two cases were diagnosed as tumor recurrence by histopathological examination. The FA value of case 3 revealed a low value in the enhanced lesion. This case was diagnosed as radiation necrosis by histopathological examination. In radiation necrosis tissue, there are no normal fibers or cell structures, and thus the directionality of water diffusion is decreased. Consequently, the FA value of radiation necrosis tissue may be lower than that of tumor recurrence (Fig. 5).

In conclusion, although our observations were limited to only three cases, they suggest that the assessment of FA value in enhanced lesions after radiotherapy may be able to differentiate radiation necrosis from tumor recurrence. This non-invasive technique will most likely become an option for auxiliary examinations for histological diagnosis after adjuvant radiotherapy. Using FA value, unnecessary craniotomies may be avoided in the future.

Acknowledgments

This work was supported in part by Grants-in-Aid for Advanced Medical Science Research by the Ministry of Education, Culture, Sports, Science, and Technology, Japan.

References

[1] Covarrubias DJ, Rosen BR, Lev MH. Dynamic magnetic resonance perfusion imaging of brain tumors. Oncologist 2004;9:528–37.

[2] Patronas NJ, Di Chiro G, Brooks RA, DeLaPaz RL, Kornblith PL, Smith BH, et al. Work in progress: [^{18}F] fluorodeoxyglucose and positron emission tomography in the evaluation of radiation necrosis of the brain. Radiology 1982;144:885–9.

[3] Tsuyuguchi N, Sunada I, Iwai Y, Yamanaka K, Tanaka K, Takami T, et al. Methionine positron emission tomography of recurrent metastatic brain tumor and radiation necrosis after stereotactic radiosurgery: is a differential diagnosis possible? J Neurosurg 2003;98:1056–64.

[4] Valk PE, Budinger TF, Levin VA, Silver P, Gutin PH, Doyle WK. PET of malignant cerebral tumors after interstitial brachytherapy. Demonstration of metabolic activity and correlation with clinical outcome. J Neurosurg 1988;69:830–8.

[5] Barai S, Bandopadhayaya GP, Julka PK, Naik KK, Haloi AK, Kumar R, et al. Role of Tc-glucoheptonic acid brain single photon emission computed tomography in differentiation of recurrent brain tumour and post-radiation gliosis. Australas Radiol 2004;48:296–301.

[6] Kline JL, Noto RB, Glantz M. Single-photon emission CT in the evaluation of recurrent brain tumor in patients treated with gamma knife radiosurgery or conventional radiation therapy. Am J Neuroradiol 1996;17:1681–6.

[7] Serizawa T, Saeki N, Higuchi Y, Ono J, Matsuda S, Yanagisawa M, et al. Diagnostic value of thallium-201 chloride single-photon emission computerized tomography in differentiating tumor recurrence from radiation injury after gamma knife surgery for metastatic brain tumors. J Neurosurg 2005;102:266–71.

[8] Rock JP, Hearshen D, Scarpace L, Croteau D, Gutierrez J, Fisher JL, et al. Correlations between magnetic resonance spectroscopy and image-guided histopathology, with special attention to radiation necrosis. Neurosurgery 2002;51:912–20.

[9] Dethy S, Goldman S, Blecic S, Luxen A, Levivier M, Hildebrand J. Carbon-11-methionine and fluorine-18-FDG PET study in brain hematoma. J Nucl Med 1994;37:1162–6.

[10] Ogawa T, Hatazawa J, Inugami A, Murakami M, Fujita H, Shimosegawa E, et al. Carbon-11-methionine PET evaluation of intracerebral hematoma: distinguishing neoplastic from non-neoplastic hematoma. J Nucl Med 1995;36:2175–9.

[11] Iwai Y, Yamanaka K, Oda J, Tsuyuguchi N, Ochi H. Tracer accumulation in radiation necrosis of the brain after thallium-201 SPECT and [11C]methionine PET-case report. Neurol Med Chir 2001;41:415–8.

[12] Sinha S, Bastin ME, Whittle IR, Wardlaw JM. Diffusion tensor MR imaging of high-grade cerebral gliomas. Am J Neuroradiol 2002;23:520–7.

[13] Beppu T, Inoue T, Shibata Y, Kurose A, Arai H, Ogasawara K, et al. Measurement of fractional anisotropy using diffusion tensor MRI in supratentorial astrocytic tumors. J Neurooncol 2003;63:109–16.

[14] Misaki T, Beppu T, Inoue T, Ogasawara K, Ogawa A, Kabasawa H. Use of fractional anisotropy value by diffusion tensor MRI for preoperative diagnosis of astrocytic tumors: case report. J Neurooncol 2004;70:343–8.

[15] Beppu T, Inoue T, Shibata Y, Yamada N, Kurose A, Ogasawara K, et al. Fractional anisotropy value by diffusion tensor magnetic reso-

nance imaging as a predictor of cell density and proliferation activity of glioblastomas. Surg Neurol 2005;63:56–61.
[16] Inoue T, Ogasawara K, Beppu T, Ogawa A, Kabasawa H. Diffusion tensor imaging for preoperative evaluation of tumor grade in gliomas. Clin Neurol Neurosurg 2005;107:174–80.
[17] Pierpaoli C, Basser PJ. Toward a quantitative assessment of diffusion anisotropy. Magn Reson Med 1996;36:893–906.
[18] Papadakis NG, Xing D, Houston GC, Smith JM, Smith MI, James MF, et al. A study of rotationally invariant and symmetric indices of diffusion anisotropy. Magn Reson Med 1999;17:881–92.
[19] Sorensen AG, Wu O, Copen WA, Davis TLGonzalez RG, Koroshetx WJ, Reese TG, et al. Human acute cerebral ischemia: detection of changes in water diffusion anisotropy by using MR imaging. Radiology 1999;212:785–92.
[20] Werring DJ, Clark CA, Parker GJ, Miller DH, Thompson AJ, Barker GJ. A direct demonstration of both structure and function in the visual system: combining diffusion tensor imaging with functional magnetic resonance imaging. Neuroimage 1999;9:352–61.
[21] Pierpaoli C, Jezzard P, Basser PJ, Barnett A, Di Chiro G. Diffusion tensor MR imaging of the human brain. Radiology 1996;201: 637–48.
[22] Witwer BP, Moftakhar R, Hasan KM, Deshmukh P, Haughton V, Field A, et al. Diffusion-tensor imaging of white matter tracts in patients with cerebral neoplasm. J Neurosurg 2002;97: 568–75.
[23] Yasargil MG, Microneurosurgery IV A (in 4 vol.). Georg Thieme, Stuttgart/New York Verlag (for distribution in Japan: Nankodo Company Ltd., Tokyo; 1993. p. 127).

ELSEVIER

Clinical Neurology and Neurosurgery 109 (2007) 327–334

Clinical Neurology and Neurosurgery

www.elsevier.com/locate/clineuro

Preoperative imaging of superficially located glioma resection using short inversion-time inversion recovery images in high-field magnetic resonance imaging

Takaaki Beppu [a,*], Takashi Inoue [a], Hideaki Nishimoto [a], Kuniaki Ogasawara [a], Akira Ogawa [a], Makoto Sasaki [b]

[a] *Department of Neurosurgery, Iwate Medical University, 19-1 Uchimau, Morioka 020-8505, Japan*
[b] *Department of Radiology, Iwate Medical University, Morioka, Japan*

Received 22 July 2006; received in revised form 26 December 2006; accepted 4 January 2007

Abstract

Objectives: Short inversion-time inversion recovery (STIR) is the only magnetic resonance imaging (MRI) sequence able to produce high contrast images of both brain-CSF and gray matter–white matter in the central nervous system. The aim of the present study is to evaluate the effectiveness of STIR in imaging tumor involvement of the cortical surface and intra-axial structures, its usefulness in the resection of superficially located gliomas.

Patients and methods: In this study, we perform conventional MRI (1.5 T) and STIR (3.0 T) before surgery in 10 patients with superficially located glioma. We estimate the spatial relationship between the tumor bulk, the adjacent cortical surface and intra-axial structures on T2WI (1.5 T) and STIR (3.0 T). STIR findings are applied to resection of the tumor in each case.

Results: For all patients, STIR provided more satisfactory images than T2WI of both the cortical surface structures and intra-axial structures surrounding the tumor. During surgery, the clear demonstration of cortical surface structures on preoperative STIR images assisted in determining tumor location and the sulci to be split for the trans-sulcal approach for patients whose cortex was normal in colour. Clear contrast on STIR between the tumor margin and peritumoral edema was useful for tumor resection.

Conclusion: STIR is able to demonstrate anatomical details of the cortical surface and intra-axial structures of the brain and is therefore suitable for the preoperative evaluation of superficially located gliomas.

Keywords: MRI; Oligodendroglial tumor; Preoperative evaluation; Short inversion-time inversion recovery; Superficially located glioma

1. Introduction

The main goal of clinical imaging is the detection of pathological lesions within a target structure at high anatomical resolution [1,2]. Routine magnetic resonance imaging (MRI) examinations are performed using a combination of contrast techniques, including T1-weighted images (T1WI), T2-weighted images (T2WI), proton density-weighted images (PDWI), diffusion-weighted images, and fluid-attenuated inversion recovery images (FLAIR). Some of these sequences exhibit poor anatomical detail of central nervous system (CNS) structures; therefore, a new MRI technique is required that is capable of accurately visualizing morphological information. Fujii et al. and Harada et al. [1,3] developed a video-inverted high-resolution PDWI, known as T2-reversed MRI (T2R) that reverses and expands the gray scale of the PDWI in a high-field MRI system. Compared with conventional MRI, T2R provides improved physiological resolution and fine contrast resolution of CNS structures due to reversal of the PDWI and improvement of the single-to-noise (S/N) ratio by using a high magnetic field system [1,3,4].

Like T2R, short inversion-time inversion recovery (STIR) imaging at high magnetic field strength has become a routine

* Corresponding author. Tel.: +80 19 651 5111; fax: +80 19 625 8799.
E-mail address: tbeppu@iwate-med.ac.jp (T. Beppu).

0303-8467/$ – see front matter © 2007 Published by Elsevier B.V.
doi:10.1016/j.clineuro.2007.01.005

MRI sequence for imaging CNS structures [2]. A STIR image with a reversed gray-scale produces an image with contrast that is similar to that of T2R. STIR is widely used as a fat-suppression technique and is used clinically for evaluating intraorbital disease, bone marrow disease, and soft-tissue disorders [5–10]. A short inversion time that leads the magnetization vector of fat tissue completely to zero suppresses the signal from fat. The short inversion time and high anatomic resolution of STIR also produces high-contrast imaging of minute CNS structures [2,11,12]. Importantly, STIR retains prominent potentials of high brain-cerebrospinal fluid (CSF) contrast as well as high white matter–gray matter (intra-axial) contrast. This potential is induced by the additive effect of proton density and T1 and T2 relaxations on the STIR signal alteration [2,7,12,13]. The S/N ratio of a STIR sequence increases within a high-field system, and it has been suggested that high-field STIR sequences should be routine in the examination of CNS diseases [2,11–13], although the usefulness of STIR in the treatment of brain tumors has yet to be investigated. The present study aims to evaluate whether STIR can be used to visualize both cortical surface structures and intra-axial structures that surround a brain tumor. We performed STIR instead of T2WI, PDWI, and FLAIR using a high field system as a routine preoperative MRI examination for patients with superficially located glioma. Here we report the findings of preoperative STIR imaging in 10 cases of superficially located glioma. The principal aim of this study is to assess the benefits of STIR as a preoperative examination for the resection of superficially located gliomas.

2. Patients and methods

2.1. Patients

Patients recruited to this study were hospitalized in the Department of Neurosurgery at Iwate Medical University, Japan, between October 2004 and October 2005. Entry criteria for this study comprised: (A) a diagnosis of superficially located glioma based on the findings of preoperative MRI; (B) tumor bulk growing and/or invading into the subcortex of the gyrus; and (C) provision of informed written consent. Superficially located glioma was defined as a tumor growing and/or invading into the subcortex of the gyrus. A total of 10 patients with newly diagnosed superficially located glioma participated in this study. All patients presented with a seizure. The patients comprised seven men and three women with an age range of 19–68 years (median age: 46 years) and diagnoses of oligodendroglioma ($n = 3$), anaplastic oligodendroglioma ($n = 5$), diffuse astrocytoma ($n = 1$), and ganglioglioma ($n = 1$) (Table 1).

Table 1
Patient summary

Case	Age	Sex	Pathology	Tumor location
1	57	M	Diffuse astrocytoma	Lt. frontal lobe
2	19	F	Ganglioglioma	Rt. temporal lobe
3	22	M	Oligodendroglioma	Lt. frontal lobe
4	36	M	Oligodendroglioma	Rt. frontal lobe
5	62	F	Oligodendroglioma	Lt. frontal lobe
6	40	M	Anaplastic oligodendroglioma	Rt. frontal lobe
7	47	M	Anaplastic oligodendroglioma	Lt. parietal lobe
8	51	F	Anaplastic oligodendroglioma	Lt. frontal lobe
9	58	M	Anaplastic oligodendroglioma	Lt. frontal lobe
10	68	M	Anaplastic oligodendroglioma	Rt. frontal lobe

2.2. Conventional MRI and STIR imaging

All patients underwent conventional MRI and STIR within 7 days prior to surgery. Conventional MRI was performed using a 1.5 T whole body scanner (Signa LX 9.1, GE Yokogawa Medical Systems, Tokyo, Japan) and a standard head coil. Conventional MRI such as T1WI, T2WI, and gadolinium-enhanced T1WI (Gd-T1WI), was performed. Imaging parameters for T2WI were as follows: repetition time (TR) 2800 ms, echo time (TE) 11 ms, matrix 256 × 256, field of view (FOV) 220 mm, and slice thickness 6 mm. STIR imaging was performed using a 3.0 T MRI system (Signa VH/i, GE Medical Systems, Milwaukee, WI, USA) and a standard head coil. The following pulse sequences were used: TR 5000 ms, TE 25 ms, inversion time 140 ms, matrix 512 × 384, FOV 240 mm, and slice thickness 6 mm. STIR images were made by gray scale inversion of the original images.

We compared the spatial relationship between cortical surface structures such as sulci, vessels, and the gyrus (gyri) involving the tumor on STIR images with T2WI that retain high brain-CSF contrast resolution on conventional MRI. We also visually compared the intra-axial contrast of the tumor margin and surrounding white matter between T2WI and STIR.

2.3. Tumor resection

To assess whether the anatomical resolution of STIR accurately depicts the anatomical structures visualized during surgery, we did not use stereotactic navigation (frame-based or frameless) for all tumor resections. During surgery, cortical surface structures were observed on the surgical field and compared with the STIR findings. In cases where the gyrus involving the tumor was normal in colour, we determined the tumor location from the STIR findings. The STIR images were used to determine the sulci to be split in order to separate the gyrus (gyri) involving the tumor from neighboring gyri. We completely split the sulci and separated the tumor bulk from adjacent normal gyri (trans-sulcal approach). The tumor was then dissected from the surrounding white matter along the tumor margin. Follow-up MRI was performed in the period between surgery and adjuvant therapy to estimate the extent and accuracy of tumor removal.

3. Results

In all patients, the STIR images using 3.0 T MRI more clearly demonstrated the cortical surface structures adjacent to the tumor bulk than conventional MRI using 1.5 T MRI. STIR findings were useful in preoperative planning for resection of the tumor, as structures such as sulci and vessels adjacent to the tumor bulk could be precisely observed on STIR prior to surgery. The STIR images enabled us to confidently determine the sulci to be split in the trans-sulcal approach. During surgery, the cortical surface was of normal colour in six patients. These patients consisted of all cases with a tumor other than anaplastic oligodendroglioma and one case of anaplastic oligodendroglioma. Preoperative STIR evaluation of the spatial relationship of the cortical surface structures between the gyrus (gyri) involving the tumor bulk, sulci, and vessels contributed to the determination of the tumor location two-dimensionally on the cortical surface in five of six patients whose cortex was a normal colour (Cases 1 and 4 described below). Only one (Case 2) of these six patients was STIR not useful for localization of the tumor on the cortical surface. In this case, there was no cortical vessel on the cortex involved with the tumor. The sulci to be separated from the adjacent normal gyri were clearly identified; however, the resection line to be dissected at the gyrus crossing the sulci could not be determined due to the lack of cortical vessels. Intraoperative ultrasound was used to determine the tumor location for this case. During surgery for patients with anaplastic oligodendroglioma, tumor location on the cortex was easily determined because the cortex of the gyrus involving the tumor was a reddish colour in four of these five patients.

In all patients, preoperative STIR differentiated the tumor margin from surrounding white matter more clearly than T2WI using conventional MRI. After splitting the sulci, the tumor was then dissected from the surrounding white matter along the demarcated tumor margin. STIR was useful for dissection of the tumor bulk: for example, in cases of anaplastic oligodendroglioma with wide spread peritumoral edema, preoperative evaluation with STIR was used to guide the direction and depth of dissection during removal of the tumor bulk and peritumoral edema, as illustrated in Case 7 described below.

3.1. Illustrative case reports

3.1.1. Case 1

In this patient, a tumor was growing in the left superficial frontal lobe. We confirmed that the speech area and the arcuate fasciculus were not involved with the tumor bulk by performing the preoperative functional MRI and diffusion-weighted three-dimensional anisotropy contrast axonography MRI. Anatomical resolution of both the cortical surface and intra-axial structures was clearer on STIR using 3.0 T MRI than on T2WI using 1.5 T MRI (Fig. 1A and B). The coronal STIR image indicated that the tumor bulk was located within the gyri between the superior frontal sulcus and the inferior frontal sulcus. In the sagittal view, a thick cortical vein was observed in a sulcus above the tumor bulk. The tumor bulk was localized preoperatively within the gyri between the first sulcus forward and the third sulcus back from this cortical vein (Fig. 1C). During surgery, we determined the tumor location on the cortex two-dimensionally from the preoperative STIR evaluation and confidently removed the tumor, even though the cortical surface was of normal colour (Fig. 1D). Postoperative STIR demonstrates the extent of tumor resection (Fig. 1E). Pathological diagnosis was diffuse astrocytoma.

3.1.2. Case 4

Preoperative STIR demonstrated the tumor growing in the cingulate gyrus, bordered by the cingulate sulcus anteriorly and the corpus callosum sulcus posteriorly. Anterior cerebral arteries were sited in the cingulate sulcus and on the surface of the genu of the callosum. These anatomical structures were demonstrated more clearly on STIR than on T2WI (Fig. 2A and B). Intra-axial structures were also clearly visualized by STIR. During surgery, sulci and vessels previously identified on STIR were observed on the cortical surface of the cerebral longitudinal fissure. The tumor was the white colour of normal cortex and could not be located on the basis of colour; however, we determined the tumor location from preoperative STIR images. We split the cingulate sulcus and corpus callosum sulcus and then excised the tumor using the trans-sulcal approach. Postoperative MRI confirmed that the tumor had been entirely removed with an exact split line (Fig. 2C). Pathological diagnosis was pure oligodendroglioma.

3.1.3. Case 7

In this case, a growing tumor enhanced by gadolinium on T1WI was observed in the left parietal lobe (Fig. 3A). The tumor was separated from the occipital lobe by the parieto-occipital sulcus, with the tumor margin located behind the lateral ventricle. These spatial relationships were visualized more clearly on STIR than on T2WI (Fig. 3B and C). Surgery was planned to preserve the left parietal lobe cortex in to avoid Gerstmann syndrome. During surgery, the parieto-occipital sulcus was easily identified by the reddish colour of the gyrus involving the tumor. We completely split the parieto-occipital sulcus and separated the tumor bulk from the occipital lobe. The tumor was then dissected from the surrounding white matter along the demarcated tumor margin. Fine contrast resolution between the tumor bulk, peritumoral edema, and surrounding normal white matter on STIR guided direction and depth during removal of tumor bulk and peritumoral edema. While edematous white matter on the anterior side of the tumor bulk was removed, the lateral ventricle was not opened despite of the tumor border proximity. Postoperative MRI showed that the tumor was successfully debulked with preservation of the parietal lobe cortex (Fig. 3D). The patient did not display Gerstmann syndrome. The pathological diagnosis was anaplastic oligodendroglioma.

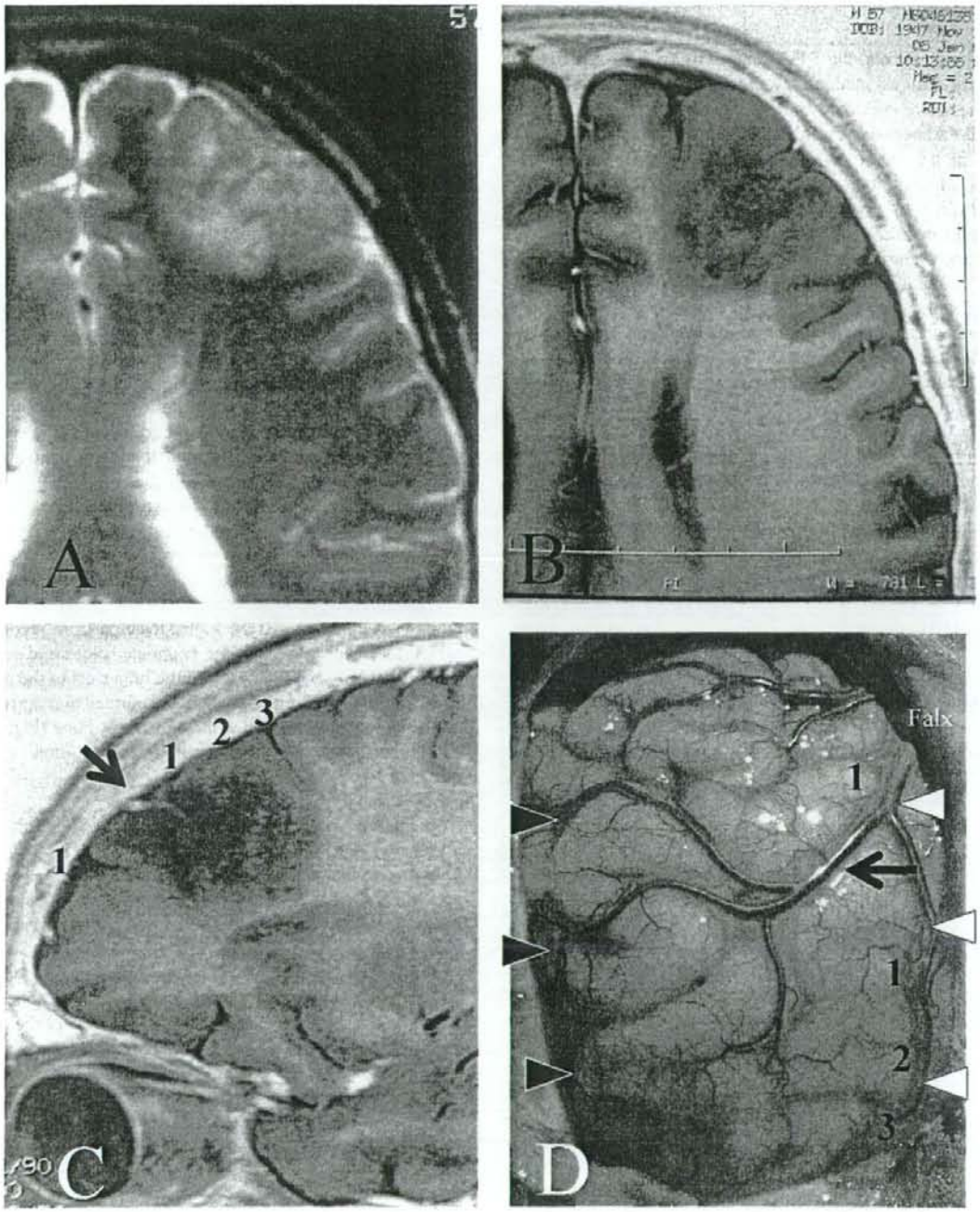

Fig. 1. Images for Case 1. The cortical vessels and sulci were visualized more clearly on axial STIR using 3.0 T MRI (B) than on T2WI using 1.5 T MRI (A). Sagittal STIR (C) demonstrates the tumor bulk located within gyri between the first sulcus forward and the third sulcus back from a cortical vein (arrow). The sulcus number is indicated with a numeral. Cortical surface showing normal colour (D). Surgical findings of a cortical vein (arrow), the superior frontal sulcus (white arrowheads), the inferior frontal sulcus (black arrowheads), and numerals showing the sulcus numbers correspond to those on the sagittal STIR image. Postoperative STIR (E) shows that the tumor has been debulked accurately, although postsurgical edema is seen in the white matter adjacent to the tumor bed.

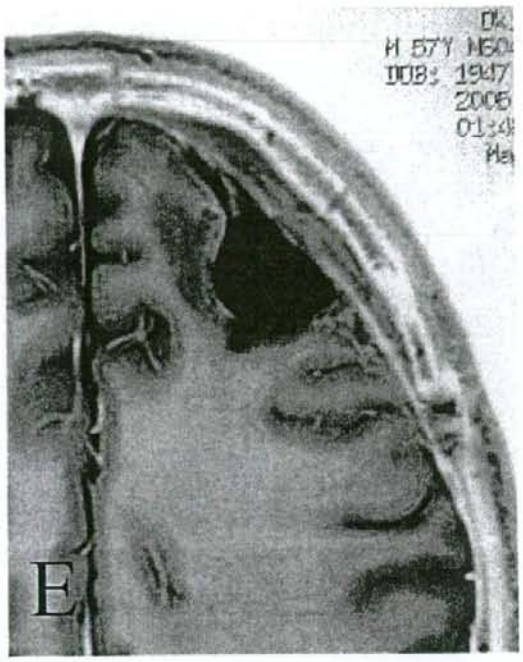

Fig. 1. (*Continued*).

4. Discussion

In the present study, the use of STIR in a high magnetic field system enabled clear depiction of the cortical surface and intra-axial structures in all patients. In particular, cortical vessels and sulci were visualized more clearly on STIR than on conventional T2WI using 1.5 T MRI. These clear depictions of STIR were beneficial for understanding the spatial relationships between the cortical surface structures, neighboring white matter, and tumor bulk. Our results confirm previous reports that STIR in a high magnetic field can produce high contrast resolution comparable to that of micro- or macroscopic specimens of the CNS [2,12]. While T2WI shows high brain-CSF contrast and low intra-axial contrast, PDWI demonstrates high intra-axial contrast and low brain-CSF contrast. The very short inversion time of STIR makes this the only sequence in which signal intensity is additively affected by proton density and T1 and T2 relaxations. This characteristic improves both the brain-CSF contrast and intra-axial contrast [2,7,12,13]. Compared with FLAIR, STIR has a higher contrast resolution because FLAIR contrast incorporates signal intensities that are competitively affected by T1 and T2 relaxation. STIR has similar appearances to reversed gray-scale T2R images in a high field MRI system. T2R provides an excellent means of elucidating the fine details of intracranial pathology [1,3]; however, T2R has excellent intra-axial contrast, although lower brain-CSF contrast than STIR. STIR is therefore superior to T2R, particularly in terms of brain-CSF contrast [12].

Tumor location can be difficult to determine without navigation tools if the cortical surface of the tumor bulk is normal in colour as demonstrated in Cases 1 and 4. The high brain-CSF contrast of preoperative STIR evaluation enables us to accurately determine the tumor location. In contrast, during surgery, the utility of STIR possesses the following limitations regarding two-dimensional localization of the tumor on the cortical surface; (i) it is necessary to have information on both the sulci and the vessels on STIR, and (ii) STIR is of limited use for most anaplastic oligodendrogliomas because the reddish cortex of patients with this tumor means that the gyri involving the tumor can be easily differentiated from the surrounding normal gyri.

The high intra-axial contrast of STIR is also useful for resection of superficially located gliomas as shown in Case 7. The high intra-axial contrast of STIR provided clear depiction of intracerebral structures, providing fine contrast between tumor tissue, peritumoral edema and surrounding normal white matter. STIR images were useful for guidance of the resection direction and depth within the white matter. Gliomas can be localized for removal using several methods that include intraoperative ultrasound, frame-based or frameless stereotactic navigation tools, intraoperative navigation that combines brain mapping and functional MRI, and intraoperative MRI [14–20]. STIR will become an optional neuroimaging technique to support these surgical methods. The present study did not use neuro-navigation to confirm the accuracy of anatomical resolution on STIR; however, the combination of STIR and a neuro-navigation system would

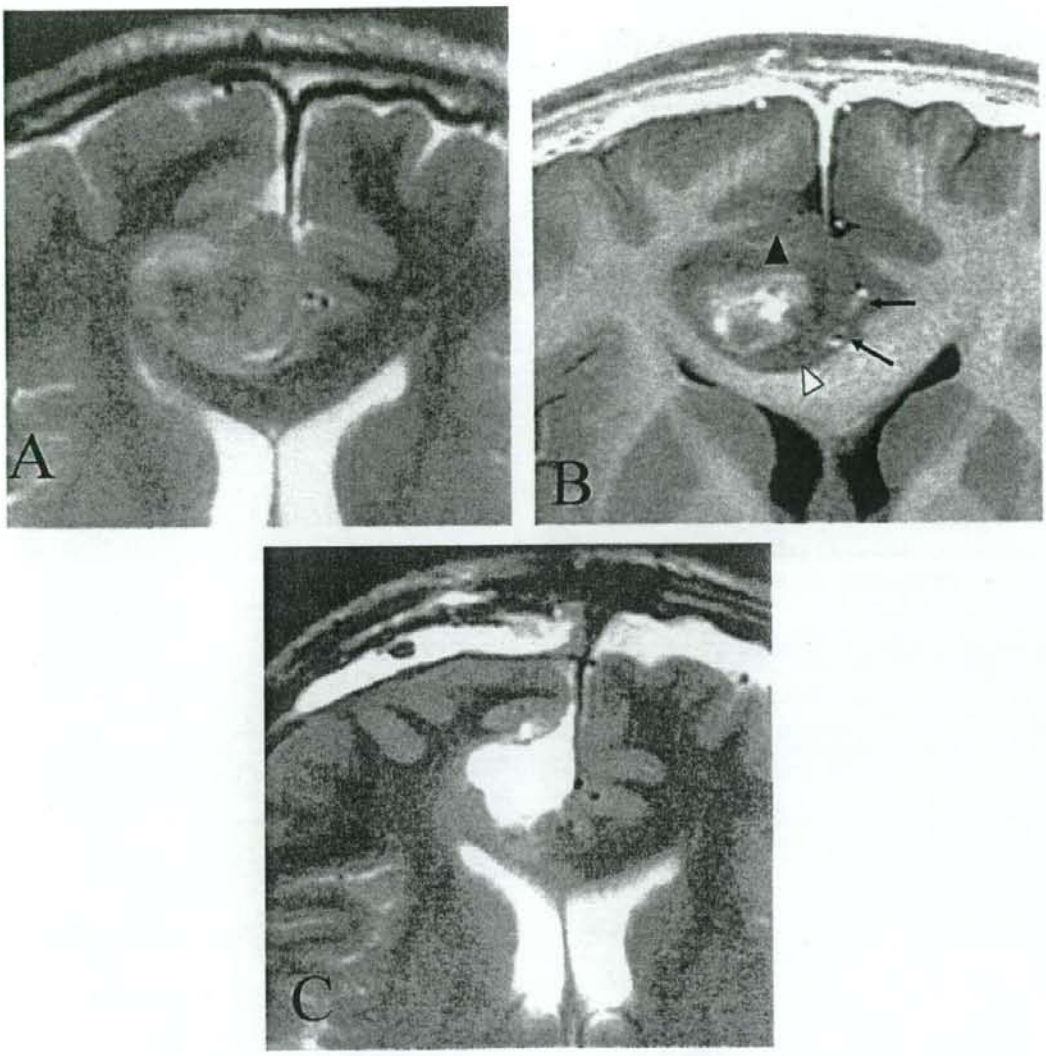

Fig. 2. Images for Case 4. Axial T2WI using 1.5 T MRI (A) and axial STIR image using 3.0 T MRI (B). Black arrowhead: the cingulate sulcus, white arrowhead: corpus callosum sulcus, arrows: the pericallosal and callosomarginal arteries. Postoperative T2WI using 1.5 T MRI (C) performed at a different hospital demonstrates satisfactory removal of the tumor bulk.

be useful for resection of tumors sited in the deep white matter.

Oligodendroglial tumor will be increasingly encountered by neurooncologists, because the morphological spectrum of oligodendroglial tumor includes tumors that have previously been misinterpreted as astrocytomas [21]. In the present study, 8 of 10 patients presented with oligodendroglial tumor. Oligodendroglial tumor is commonly seen as a superficially located, clearly demarcated tumor enlarging a single gyrus [15,22]. MRI typically demonstrates that oligodendroglial tumor appears well-demarcated and shows little peritumoral edema [23]. Peritumoral edema must be removed as completely as possible to prevent microscopic infiltration of the tumor into surrounding edematous brain tissue [24]. Gross total removal has been recognized as a prognostic factor in oligodendroglial tumors [25–30]; however, a previously report states that extensive gross total removal, such as lobectomy, is not a prognostic factor [30]. For these reasons, it is important to accurately remove superficially located cerebral oligodendroglial tumors while minimizing injury to the surrounding brain. The trans-sulcal approach is commonly used as a standard strategy when removing a glioma to minimize invasion into the brain [31]. Clear anatomical resolution of the cortical surface on STIR images helps to identify the sulci